IEEE Photonics Journal
An IEEE Photonics Society Publication

Open Access

Tunable Passively-Synchronized 1-μm Q-Switched and 1.5-μm Gain-Switched Dual-Wavelength Fiber Laser Based on an Er/Yb Codoped Fiber

Volume 9, Number 3, June 2017

Chunyu Guo
Weiqi Liu
Shuangchen Ruan
Jun Yu
Yewang Chen
Peiguang Yan
Jinzhang Wang
Saurabh Jain
Ping Hua

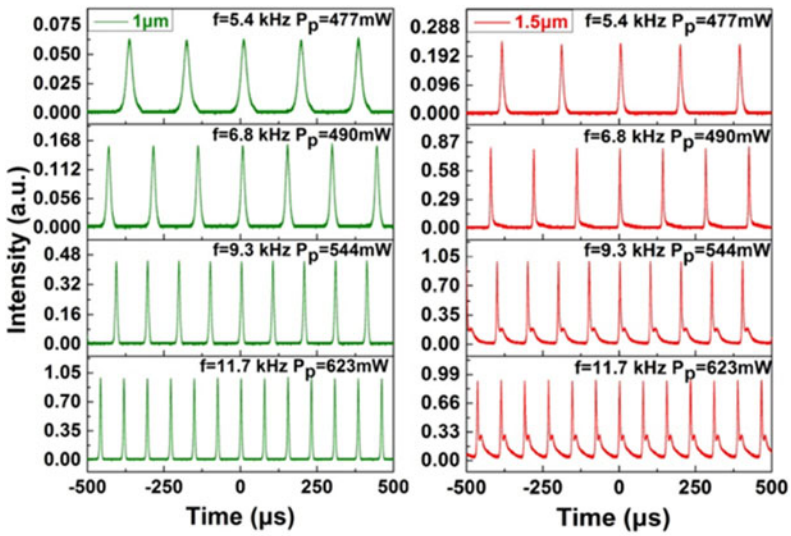

DOI: 10.1109/JPHOT.2017.2687940
1943-0655

Tunable Passively-Synchronized 1-μm Q-Switched and 1.5-μm Gain-Switched Dual-Wavelength Fiber Laser Based on an Er/Yb Codoped Fiber

Chunyu Guo,[1,2] Weiqi Liu,[1] Shuangchen Ruan,[1] Jun Yu,[1] Yewang Chen,[1] Peiguang Yan,[1] Jinzhang Wang,[1] Saurabh Jain,[2] and Ping Hua[2]

[1]Shenzhen Key Laboratory of Laser Engineering, Key Laboratory of Advanced Optical Precision Manufacturing Technology of Guangdong Higher Education Institutes, College of Optoelectronic Engineering, College of Electronic Science and Technology, Shenzhen University, Shenzhen 518060, China
[2]Optoelectronics Research Centre, University of Southampton, Southampton SO17 1BJ, U.K.

DOI:10.1109/JPHOT.2017.2687940

Manuscript received January 13, 2017; revised March 20, 2017; accepted March 21, 2017. Date of current version April 21, 2017. This work was supported in part by the National Natural Science Foundation of China under Grant 61308049; in part by the National High-tech R&D Program of China (863 Program) under Grant 2015AA021102; in part by the Outstanding Young Teacher Cultivation Projects in Guangdong Province under Grant YQ2015142; and in part by the Shenzhen Science and Technology Project under Grant JCYJ20160520161351540 and Grant JCYJ 20160427105041864. Corresponding author: Shuangchen Ruan (e-mail: scruan@szu.edu.cn).

Abstract: A wavelength-tunable passively-synchronized 1-μm Q-switched and 1.5-μm gain-switched dual-wavelength pulsed fiber laser has been demonstrated with a single gain fiber for the first time to our knowledge. The realized dual-wavelength co-oscillation is based on a dual ring-cavity configuration with a common Er/Yb co-doped fiber (EYDF). The Q-switched 1-μm pulses are generated through the saturable absorption effect of unpumped EYDF aided by a 1.5-μm oscillation cavity, whereas the 1.5-μm pulses are produced by the gain-switching of Er^{3+} ions induced by the 1-μm Q-switched pulses. A tuning range of 11.7 nm from 1045.3 to 1057 nm and 29.7 nm from 1535 to 1564.7 nm are obtained at stable synchronized pulse operation for 1 and 1.5-μm spectral bands, respectively.

Index Terms: Fiber lasers, pulsed lasers, dual-wavelength laser, Q-switching, gain-switching, Er/Yb co-doped fiber.

1. Introduction

Dual-wavelength lasers, especially synchronized dual-wavelength pulsed lasers with large pulse energy and high peak power, are required in many applications such as nonlinear frequency conversion [1], [2], pump-probe spectroscopy [3] and Raman scattering spectroscopy [4]. The synchronized dual-wavelength mode-locked lasers operating at the same repetition rate have been demonstrated using different methods: active synchronization where electronic feedback is applied to control the cavity length [5] and passive synchronization based on various mechanisms such as cross-phase modulation (XPM) [6], [7] and cross-absorption modulation (XAM) [8], [9]. In

comparison, passive synchronization can tolerate relatively large cavity mismatch and produce pulses with low timing jitter. Compared with solid-state lasers, fiber lasers have many attractive characteristics including compactness, environmental stability, good heat dissipation, high efficiency and excellent beam quality. Consequently, passively synchronized dual-wavelength pulsed fiber lasers have attracted considerable attention in recent years.

Passively synchronized dual-wavelength pulsed fiber lasers have been demonstrated previously using a single rare-earth doped gain medium [10]–[13], which leads to narrowly separated wavelengths and limited wavelength tunability. In order to overcome these limitations, two gain media have also been exploited to develop the synchronized dual-wavelength pulsed fiber lasers with wide wavelength separation. In 2004, Rusu *et al.* presented, for the first time, a passively synchronized 1/1.5 μm dual-wavelength mode-locked fiber laser based on two gain fibers that were cascaded to share the same cavity [14]. Zhang *et al.* demonstrated passive synchronization of an Yb and Er doped mode-locked fiber lasers using a common carbon nanotube saturable absorber (SA) in 2011 [15]. Later on, Sotor *et al.* successfully demonstrated passive synchronization of Er and Tm doped mode-locked fiber lasers using a common graphene SA in 2014 [16]. However, the above approaches of generating passively synchronized mode-locked fiber lasers require precise control of the cavity lengths significantly increasing complexity of the system. In contrast, passive synchronization in the Q-switching regime becomes less susceptible to the cavity length mismatch. In addition, the passively synchronized Q-switched fiber laser has significant advantages such as high pulse energy, variable repetition rate and better wavelength tunability. In 2014, based on a common graphene SA, passively synchronized Q-switching at 1.06 μm with a Yb doped fiber and at 1.53 μm with an Er/Yb co-doped fiber (EYDF) was reported by Wu *et al.* [17]. Recently, Cheng *et al.* obtained a dual-wavelength passively-synchronized Q-switched Tm doped fluoride fiber laser at 1.48 μm and 1.85 μm using a common graphene SA [18].

Despite these extensive developments, it is anticipated that a widely separated dual-wavelength laser based on a single gain medium would be more efficient and attractive proposition. Cascade transitions of rare-earth ion is one way to generate a number of distinct emission wavelengths simultaneously, however, such a scheme relies heavily on host materials that support less energetic phonons [19]. In recent years, using Ho-doped fluoride fiber, Li *et al.* have realized a dual-wavelength synchronized 2 μm and 3 μm Q-switched fiber laser based on cascade transitions of Ho^{3+} ions [20] and then obtained synchronized Q-switched 3 μm and gain-switched 2 μm pulses by Q-switching one of the cascade transitions thus modulating the adjacent transition to produce gain-switched pulses [21], [22]. Another way to obtain simultaneous lasing at two widely separated wavelengths is the use of a single gain medium doped with two or more different rare-earth ions [19]. Depending on the co-seeding or co-oscillating of the laser oscillation at 1 μm [23]–[26], it is possible to obtain simultaneous continuous wave (CW) operation at 1 μm and 1.5 μm using a length of EYDF [27], [28]. However, until now there is no relevant reports on 1/1.5 μm synchronized dual-wavelength pulsed fiber laser based on a single gain medium including EYDFs.

In this paper, we report an all-fiber dual-wavelength passively-synchronized 1 μm Q-switched and 1.5 μm gain-switched fiber laser based on an EYDF. The 1 μm Q-switched pulse results from the saturable absorption effect of unpumped EYDF aided by a 1.5 μm oscillation cavity, whereas 1.5 μm gain-switched pulses are induced by the 1 μm Q-switched pulses. In addition, this synchronized dual-wavelength pulsed fiber laser shows good wavelength tunability over the respective spectral bands, which is independent of each other.

2. Experimental Setup

The experimental setup of the all-fiber dual-wavelength passively-synchronized pulsed fiber laser is shown in Fig. 1 including a simplified energy level diagram of Er^{3+} and Yb^{3+} ions. As the absorption cross section for Yb^{3+} ions at the pump wavelength (975 nm) is much higher than that for Er^{3+} ions, most of the pump light is absorbed by Yb^{3+} ions, and excited to the $^2F_{5/2}$ state. Due to the well-known "bottlenecking" effect of the Yb-Er energy transfer in the EYDF with high pump absorption coefficient [29], population inversion of Yb^{3+} ions leads to two phenomena. One of them is a resonant

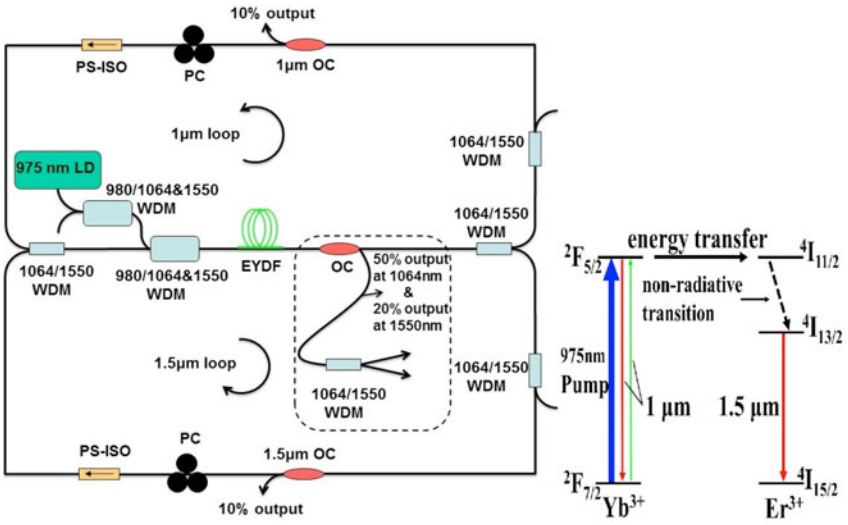

Fig. 1. Schematic of the experimental setup. Included is a simplified energy level diagram of Er^{3+} and Yb^{3+} ions.

non-radiative energy transfer to the $^4I_{11/2}$ level of Er^{3+} ions, followed by a quick non-radiative transition to the $^4I_{13/2}$ state inducing population inversion of Er^{3+} ions and a consequent laser emission at 1.5 μm. Another one is the emission at 1μm, which can be reabsorbed as a secondary pump for 1.5 μm emission [29], [30]. The setup consists of two loop resonators with one common branch including a 1.7 m long single-clad high concentration erbium/ytterbium co-doped fiber (EYDF) with the absorption coefficients of 1335 dB/m at 975 nm. A 975-nm single-mode laser diode (LD) with a maximum output power of 623 mW was used as the pump, which was coupled to the cavity with two in-house fabricated 980/1064&1550 nm wavelength division multiplexers (WDMs) connected in series. The 980/1064&1550 nm WDM ensures the coupling of both wavebands in the common branch. The additional WDM was used to protect the LD from any backward travelling 1 μm and 1.5 μm radiations. Both signals were combined and separated through two fused 1064/1550 nm WDMs. Additional two 1064/1550 nm WDMs were employed in each loop to remove 1 μm and 1.5 μm residual lasers ensuring the stability of each cavity. A polarization sensitive isolator (PS-ISO) was used in each loop to ensure co-propagation of the two laser signals in the common branch, whilst a polarization controller (PC) was used to change intra-cavity birefringence and optimize the laser output from each cavity. The PC together with the PS-ISO served as a polarizer, was also utilized to provide the birefringence-induced filtering effect to realize wavelength-tunable pulses. A 10/90 fiber output coupler (OC) was used in each loop to couple out 10% power at 1 μm and 1.5 μm respectively, and each loop has the same cavity length of $\sim$15.7 m.

Initial measurements for the dual-wavelength pulses were performed with the aforementioned setup. Then, the OC in each cavity was removed, and an OC with 50% output at 1064 nm and 20% output at 1550 nm together with a 1064/1550 nm WDM was inserted into the common branch to explore the relationship between the dual-wavelength pulses.

The laser output was observed using an optical spectrum analyzer (OSA, YOKOGAWA AQ6370B), a 1 GHz digital phosphor oscilloscope (Tektronix DPO 7014C), a 3 GHz RF-spectrum analyzer (Agilent, N9320A), and a photoelectric detector (Newport, D-100ir Detector 100 ps·950-1650 nm).

3. Result and Discussion

Fig. 2 shows the simultaneously observed stable synchronized pulses at 1 μm and 1.5 μm with the increase of pump power. The repetition rates remained the same for both pulses and could be tuned

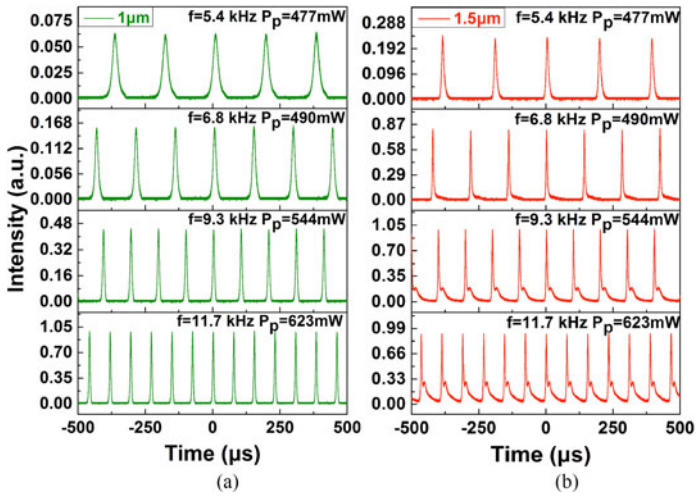

Fig. 2. Oscilloscope traces of synchronized (a) 1 μm and (b) 1.5 μm pulse trains under different pump powers: 477, 490, 544, and 623 mW.

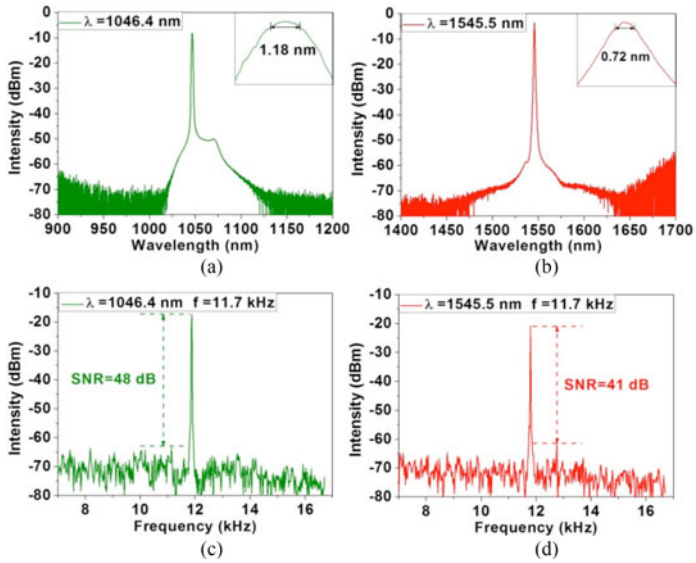

Fig. 3. Optical spectra and corresponding RF spectra of (a), (c) 1 μm and (b), (d) 1.5 μm pulses at the maximum pump power of 623 mW.

simultaneously from 5.4 to 11.7 kHz by varying the pump power from 477 to 623 mW. Compared with the 1 μm pulses, the 1.5 μm pulses at higher pump power were accompanied by a tail.

At the maximum available pump power of 623 mW, the 3-dB linewidths of the two synchronized pulses centered at 1046.4 nm and 1545.5 nm were 1.18 nm and 0.72 nm, respectively, as shown in Fig. 3(a) and (b). Corresponding RF spectra with signal-to-noise ratios (SNR) of 48 dB and 41 dB are exhibited in Fig. 3(c) and (d), respectively, indicating that both synchronized pulses are stable.

Fig. 4 shows the pulse duration and the corresponding pulse energy at 1 μm and 1.5 μm as a function of the incident pump power. With the increase in pump power, the pulse duration at 1 μm decreased whilst the pulse energy increased monotonically. Similarly, in the case of 1.5 μm signal, pulse energy increased monotonically while the pulse duration shortened initially and then remained nearly constant with the increase in pump power. At the maximum pump power of 623 mW, the

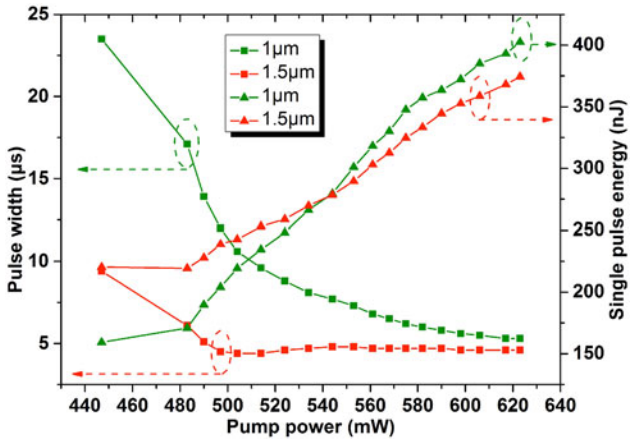

Fig. 4. Pulse width and single pulse energy at 1 μm and 1.5 μm as a function of the incident pump power.

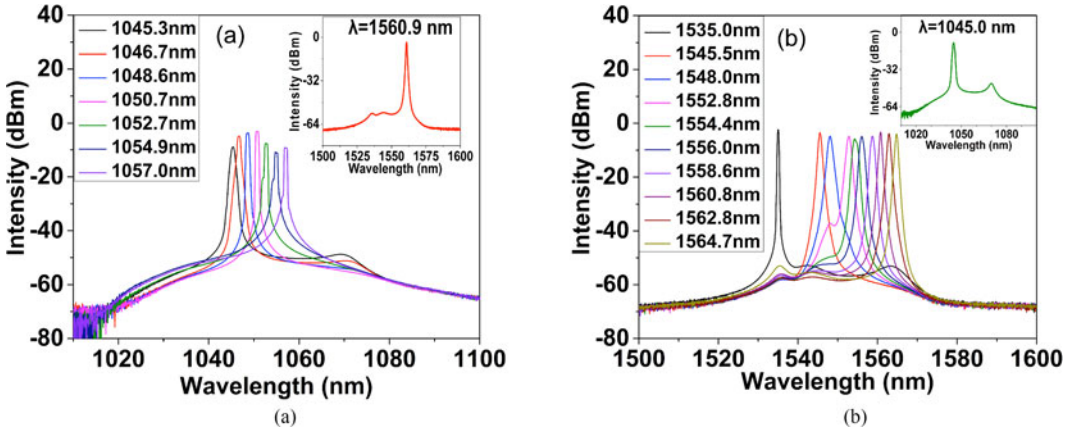

Fig. 5. Spectral tuning of (a) 1 μm and (b) 1.5 μm pulses when the other wavelength at 1.5 and 1 μm fix at 1560.9 and 1045 nm, respectively, displayed as insets.

pulse duration, single pulse energy and maximum average output power for 1 μm pulses were 5.3 μs, 402.6 nJ and 4.7 mW respectively, whereas, they were 4.6 μs, 374.4 nJ and 4.4 mW, respectively, for 1.5 μm pulses.

Furthermore, the wavelength tunability of 1 μm and 1.5 μm synchronized pulses was also demonstrated through fine-tuning of the PC orientation in their respective loop. As shown in Fig. 5(a), the center wavelength of 1 μm pulses could be tuned from 1045.3 to 1057 nm with the 1.5 μm pulses centered at 1560.9 nm at the maximum pump power. Similarly, a tuning range of 29.7 nm from 1535 to 1564.7 nm was obtained with the 1 μm pulses centered at 1045 nm, as shown in Fig. 5(b). This wavelength tunability is attributed to the birefringence-induced filtering effect [31], [32]. It was observed that the pulse intensities at different wavelengths were varied with the orientations of the PCs. It is because the transmission function of the laser cavity with respect to wavelength is related to the orientation of the PCs. It is worth noting that the orientation of the PC in one cavity did not change the operating wavelength of the other cavity, but made an impact on the output power due to gain competition [27].

The relationship between the dual-wavelength pulses was explored using the modified setup as shown by the dashed frame in Fig. 1. Two stable synchronized pulse trains at the repetition frequency of 4.8 kHz with a time delay of $\sim$26 μs were observed at a pump power of 544 mW, as shown in

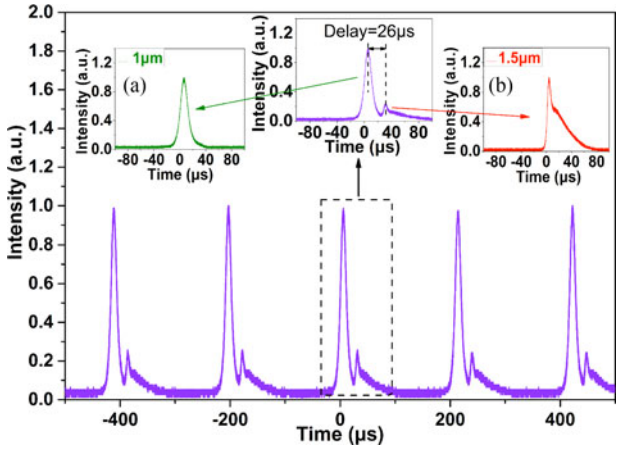

Fig. 6. Synchronized 1 μm and 1.5 μm pulse trains in the common branch when pump power is 544 mW. (Insets) (a) 1 μm single pulse. (b) 1.5 μm single pulse.

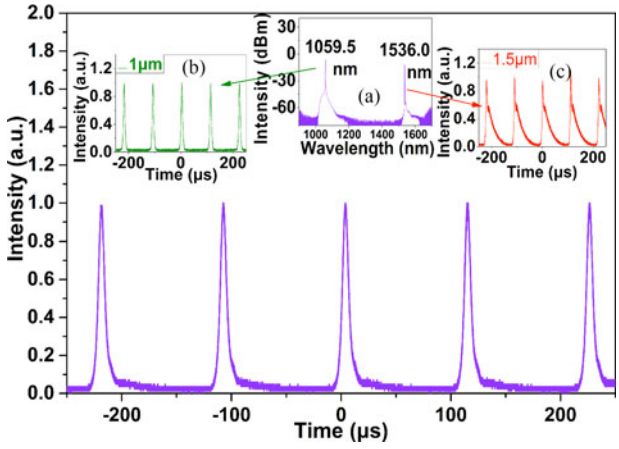

Fig. 7. Synchronized 1 μm and 1.5 μm pulse trains in the common branch when pump power is 623 mW. (Insets) (a) Combined optical spectrum. (b) 1 μm pulse train. (c) 1.5 μm pulse train.

Fig. 6. The insets (a) and (b) shows the 1 μm and 1.5 μm pulses separated by a 1064/1550 nm WDM, and it could be seen that the 1.5 μm pulses lagged behind the 1 μm pulses. In addition, the time delay between the two pulse trains gradually decreased with the increase in pump power and finally overlapped at a pump power of 623 mW, as shown in Fig. 7. The corresponding pulse repetition frequency was 9.0 kHz. The combined optical spectrum with two central wavelengths of 1059.5 nm and 1536.0 nm is depicted by the inset (a). Insets (b) and (c) show pulse trains at 1 μm and 1.5 μm, respectively.

The decrease in time delay between the two synchronized pulses with increasing pump power has similarly been observed between Q-switched and Q-switched induced gain-switched pulses in two-transition cascade fiber lasers [21], [22] and the fiber saturable absorber (FSA) based dual-cavity fiber laser [33]. Furthermore, in our experiment, it was observed that in the case of dual-wavelength synchronized pulse operation, no pulse generated from the other loop if either of the loop cavity was disconnected, which is also believed to be a natural consequence of the mutual induction between the dual-wavelength pulses for FSA-based dual-cavity fiber lasers [33], [34]. Accordingly, the following qualitative experiments were carried out to find out the exact types and the synchronization mechanism of the 1 μm and 1.5 μm pulses.

First, both PS-ISOs in the two cavities were replaced by two polarization insensitive isolators (PI-ISOs) and the synchronized pulses were still observed at a suitable pump power and PC orientations. Considering that there is no SA or polarized element in either cavity in this condition, it could be indicated that both of the dual-wavelength pulses cannot be attributed to nonlinear polarization rotation (NPR) effect but result from the possible self Q-switching or gain-switching. To ascertain further, two variable attenuators (VAs) with a maximum loss of 60 dB were inserted in the two loops to adjust the loss of each cavity, while the PCs in each loops were removed. It was found that the repetition rates of both 1 μm and 1.5 μm pulses reduced simultaneously with the increase of 1 μm cavity loss but increased with the increase of 1.5 μm cavity loss. The decrease of the repetition rate with the increase of cavity loss is a typical feature of Q-switched pulsed lasers. This suggests that the 1 μm pulses may be caused by the saturable absorption effect from the unpumped EYDF, which is similar to the self Q-switched Yb doped fiber laser studied extensively [35]. Furthermore, when the 1.7 m EYDF was cut to 0.3 m length, there were only higher-power CW outputs rather than pulsed outputs for both 1 μm and 1.5 μm oscillations, which confirms that 1 μm Q-switched pulses are generated by the unpumped EYDF serving as a FSA [36]. However, simultaneous increase of both 1 μm and 1.5 μm pulse repetition rates with the increase of 1.5 μm cavity loss indicates that the 1.5 μm pulse was not caused by Q-switching but probably a consequence of Q-switched induced gain-switching.

The progress of the self Q-switching and corresponding Q-switched induced gain-switching can be explained as follows. As the absorption coefficient of EYDF at 975 nm is 1335 dB/m, nearly all the pump was absorbed after passing through a very short length of the EYDF. In fact, there is no residual pump light after 0.3 m of EYDF even at the maximum pump power (623 mW), which was also observed experimentally. Therefore, at least 1.4 m unpumped EYDF serves as a SA to generate the 1 μm Q-switched pulses. With the generation of 1 μm Q-switched pulses and the subsequent reabsorption by Yb^{3+} ions, the population inversion of Yb^{3+} ions changes periodically, which then periodically modulates the population inversion of Er^{3+} ions through the resonant non-radiative energy transfer process. This results in the 1.5 μm gain-switched pulses, which is similar in nature to the gain-switched EYDF lasers with pulsed pumping at 900 and 975 nm [37], [38]. Moreover, the 1.5 μm pulses in our experiment were accompanied by a tail, which is a feature usually observed for gain-switched pulses [39].

With this insight many of the experimental observations could be understood. The simultaneous decrease of repetition rates for 1 μm and 1.5 μm pulses with increasing 1 μm cavity loss is attributed to the lower intra-cavity power in the 1 μm cavity and thereby the decreasing bleaching rate of the FSA. However, increasing the 1.5 μm cavity loss reduces the depopulation rate of the Er^{3+} ions and therefore the energy transfer rate from Yb^{3+} to Er^{3+} ions. Consequently, increasing Yb^{3+} population in the upper energy state raises the 1 μm intra-cavity power and accordingly increases the bleaching rate of the FSA, resulting in an increase in 1 μm repetition rate accompanied by the increasing repetition rate of the 1 μm pulse induced 1.5 μm gain-switched pulses. It is worth noting that when 1.5 μm cavity loss was too high to generate 1.5 μm oscillation, 1 μm Q-switched pulses cannot be observed under any pump power or any attenuation in the 1 μm cavity, the reason for which could be explained as follows. On one hand, the reduced energy transfer from Yb^{3+} to Er^{3+} ions due to the high 1.5 μm cavity loss and the resulting high population inversion of Yb^{3+} ions limits the reabsorption at 1 μm from the unpumped EYDF-based FSA. On the other hand, if the 1.5 μm cavity loss is too high to lase, the unpumped EYDF-based FSA would have a long relaxation time of $\sim$10 ms, lifetime of the excited state $^4I_{13/2}$ of Er^{3+}, which is much longer than the period between the possible 1 μm Q-switched pulses with several kHz repetition rate. As a result, the unpumped EYDF could not serve as an effective FSA in this case [33], [34].

4. Conclusion

In this paper, we have demonstrated, for the first time, a passively-synchronized 1 μm Q-switched and 1.5 μm gain-switched dual-wavelength pulsed fiber laser using a single piece of Er/Yb co-doped gain fiber. The synchronized dual-wavelength pulses have a tuning range of 11.7 nm and

29.7 nm for the 1 μm and 1.5 μm wavebands, respectively. The 1 μm Q-switched pulse is attributed to the saturable absorption effect from the unpumped EYDF aided by the 1.5 μm laser cavity, which ensures higher absorption and shorter relaxation time for the unpumped EYDF-based FSA. Meanwhile, the generation and reabsorption of 1 μm Q-switched pulses periodically modulates the gain of the 1.5 μm cavity resulting in the 1.5 μm gain-switched pulses synchronized to the 1 μm Q-switched pulses. It is believed that this tunable passively-synchronized dual-wavelength pulsed fiber laser should be well-suited for many potential applications such as difference- and sum-frequency generation.

Acknowledgment

The authors would like to thank Dr. S.-U. Alam and Prof. J. Sahu for useful discussion.

References

[1] F. Zhu, H. Hundertmark, A. A. Kolomenskii, J. Strohaber, R. Holzwarth, and H. A. Schuessler, "High-power mid-infrared frequency comb source based on a femtosecond Er:Fiber oscillator," *Opt. Lett.*, vol. 38, no. 13, pp. 2360–2362, Jul. 2013.
[2] D. Bouyge, A. Crunteanu, V. Couderc, D. Sabourdy, and P. Blondy, "Synchronized tunable Q-Switched fiber lasers using deformable achromatic microelectromechanical mirror," *IEEE Photon. Technol. Lett.*, vol. 20, no. 12, pp. 991–993, Jun. 2008.
[3] C. Manzoni, D. Polli, and G. Cerullo, "Two-color pump-probe system broadly tunable over the visible and the near infrared with sub-30 fs temporal resolution," *Rev. Sci. Instrum.*, vol. 77, no. 2, Feb. 2006, Art. no. 023103.
[4] F. Ganikhanov, C. L. Evans, B. G. Saar, and X. S. Xie, "High-sensitivity vibrational imaging with frequency modulation coherent anti-stokes raman scattering (FM CARS) microscopy," *Opt. Lett.*, vol. 31, no. 12, pp. 1872–1874, Jun. 2006.
[5] T. R. Schibli *et al.*, "Attosecond active synchronization of passively mode-locked lasers by balanced cross correlation," *Opt. Lett.*, vol. 28, no. 11, pp. 947–949, Jan. 2003.
[6] Z. Wei, Y. Kaboyashi, and K. Torizuka, "Passive synchronization between femtosecond Ti:Sapphire and Cr:Forsterite lasers," *Appl. Phys. B*, vol. 74, no. 1, pp. s171–s176, Jun. 2002.
[7] Y. Dai *et al.*, "Ultralow-jitter passive timing stabilization of a mode-locked Er-doped fiber laser by injection of an optical pulse train," *Opt. Lett.*, vol. 31, no. 22, pp. 3243–3245, Nov. 2006.
[8] M. Yan, W. Li, Q. Hao, Y. Li, and H. Zeng, "Square nanosecond Yb-and Er-doped fiber lasers passively synchronized to a Ti: sapphire laser based on cross-absorption modulation," *Opt. Lett.*, vol. 34, no. 13, pp. 2018–2020, Jul. 2009.
[9] M. Yan *et al.*, "High-Power nanosecond ytterbium-doped fiber laser passively synchronized with a femtosecond Ti: Sapphire laser," *Opt. Lett.*, vol. 34, no. 21, pp. 3331–3333, Nov. 2009.
[10] Z. Luo *et al.*, "Graphene-based passively Q-switched dual-wavelength erbium-doped fiber laser," *Opt. Lett.*, vol. 35, no. 21, pp. 3709–3711, Nov. 2010.
[11] Z. T. Wang, Y. Chen, C. J. Zhao, and H. Zhang, "Switchable dual-wavelength synchronously Q-switched erbium-doped fiber laser based on graphene saturable absorber," *IEEE Photon. J.*, vol. 4, no. 3, pp. 869–876, Jun. 2012.
[12] H. Zhang, D. Tang, L. Zhao, and X. Wu, "Dual-wavelength domain wall solitons in a fiber ring laser," *Opt. Exp.*, vol. 19, no. 4, pp. 3525–3530, Feb. 2011.
[13] S. Huang, Y. Wang, P. Yan, J. Zhao, H. Li, and R. Lin, "Tunable and switchable multi-wavelength dissipative soliton generation in a graphene oxide mode-locked Yb-doped fiber laser," *Opt. Exp.*, vol. 22, no. 10, pp. 11417–11426, May. 2014.
[14] M. Rusu, R. Herda, and O. G. Okhotnikov, "Passively synchronized erbium (1550-nm) and ytterbium (1040-nm) mode-locked fiber lasers sharing a cavity," *Opt. Lett.*, vol. 29, no. 19, pp. 2246–2248, Oct. 2004.
[15] M. Zhang, E. J. R. Kelleher, A. S. Pozharov, E. D. Obraztsova, S. V. Popov, and J. R. Taylor, "Passive synchronization of all-fiber lasers through a common saturable absorber," *Opt. Lett.*, vol. 36, no. 20, pp. 3984–3986, Oct. 2011.
[16] J. Sotor *et al.*, "Passive synchronization of erbium and thulium doped fiber mode-locked lasers enhanced by common graphene saturable absorber," *Opt. Exp.*, vol. 22, no. 5, pp. 5536–5543, Mar. 2014.
[17] D. Wu *et al.*, "Passive synchronization of 1.06- and 1.53- μm fiber lasers Q-switched by a common graphene SA," *IEEE Photon. Technol. Lett.*, vol. 26, no. 14, pp. 1474–1477, Jul. 2014.
[18] C. Jia *et al.*, "Passively synchronized Q-switched and simultaneous mode-locked dual-band Tm3+:ZBLAN fiber laser at 1.48- and 1.85- μm using common graphene saturable absorber," in *Proc. Conf. Adv. Photon. Congress*, 2016, Paper SoTu1G.4.
[19] B. M. Walsh, "Dual wavelength lasers," *Laser Phys.*, vol. 20, no. 3, pp. 622–634, Feb. 2010.
[20] J. Li, T. Hu, and S. D. Jackson, "Dual wavelength Q-switched cascade laser," *Opt. Lett.*, vol. 37, no. 12, pp. 2208–2210, Jun. 2012.
[21] J. Li, T. Hu, and S. D. Jackson, "Q-switched induced gain switching of a two-transition cascade laser," *Opt. Exp.*, vol. 20, no. 12, pp. 13123–13128, Jun. 2012.
[22] J. Li *et al.*, "Mid-infrared passively switched pulsed dual wavelength Ho^{3+}-doped fluoride fiber laser at 3 μm and 2 μm," *Sci. Rep.*, vol. 5, Jun. 2015, Art. no. 10770.
[23] K. Krzempek, G. Sobon, J. Sotor, and K. M. Abramski, "Fully-integrated dual-wavelength all-fiber source for mode-locked square-shaped mid-IR pulse generation via DFG in PPLN," *Opt. Exp.*, vol. 23, no. 25, pp. 32080–32086, Dec. 2015.

[24] V. Kuhn, P. Weßels, J. Neumann, and D. Kracht, "Stabilization and power scaling of cladding pumped Er:Yb-codoped fiber amplifier via auxiliary signal at 1064 nm," *Opt. Exp.*, vol. 17, no. 20, pp. 18304–18311, Sep. 2009.
[25] D. Ouyang, C. Guo, S. Ruan, P. Yan, H. Wei, and J. Luo, "Yb band parasitic lasing suppression in Er/Yb-co-doped pulsed fiber amplifier based on all-solid photonic bandgap fiber," *Appl. Phys. B*, vol. 114, no. 4, pp. 585–590, Jul. 2013.
[26] Q. Han, Y. He, Z. Sheng, W. Zhang, J. Ning, and H. Xiao, "Numerical characterization of Yb-signal-aided cladding-pumped Er:Yb-codoped fiber amplifiers," *Opt. Lett.*, vol. 36, no. 9, pp. 1599–1601, May. 2011.
[27] J. Boullet *et al.*, "Tunable red light source by frequency mixing from dual band Er/Yb co-doped fiber laser," *Opt. Exp.*, vol. 14, no. 9, pp. 3936–3941, May. 2006.
[28] Z. Jusoh *et al.*, "Dual-wavelength erbium-ytterbium co-doped fibre laser operating at 1064 and 1534 nm," *Ukr. J. Phys. Opt.*, vol. 15, no. 3, pp. 118–122, May. 2014.
[29] Q. Han, J. Ning, and Z. Sheng, "Numerical investigation of the ASE and power scaling of Cladding-Pumped Er–Yb codoped fiber amplifiers," *IEEE J. Quantum Electron.*, vol. 46, no. 11, pp. 1535–1541, Nov. 2010.
[30] Q. Han, Y. Yao, Y. Chen, F. Liu, T. Liu, and H. Xiao, "Highly efficient Er/Yb-codoped fiber amplifier with an Yb-band fiber bragg grating," *Opt. Lett.*, vol. 40, no. 11, pp. 2634–2636, Jun. 2015.
[31] H. Lin, C. Guo, S. Ruan, and J. Yang, "Tunable and switchable dual-wavelength dissipative soliton operation of a weak birefringence all-normal-dispersion Yb-doped fiber laser," *IEEE Photon. J.*, vol. 5, no. 5, Oct. 2013, Art. no. 1501807.
[32] H. Lin, C. Guo, S. Ruan, and J. Yang, "Dissipative soliton resonance in an all-normal-dispersion Yb-doped figure-eight fibre laser with tunable output," *Laser Phys. Lett.*, vol. 11, no. 8, Jun. 2014, Art. no. 085102.
[33] T. Y. Tsai, Y. C. Fang, H. M. Huang, H. X. Tsao, and S. T. Lin, "Saturable absorber Q- and gain-switched all-Yb3+ all-fiber laser at 976 and 1064 nm," *Opt. Exp.*, vol. 18, no. 23, pp. 23523–23528, Nov. 2010.
[34] V. V. Dvoyrin, V. M. Mashinsky, and E. M. Dianov, "Yb-Bi pulsed fiber lasers," *Opt. Lett.*, vol. 32, no. 5, pp. 451–453, Mar. 2007.
[35] A. V. Kir'Yanov and Y. O. Barmenkov, "Self-Q-switched Ytterbium-doped all-fiber laser," *Laser Phys. Lett.*, vol. 3, no. 10, pp. 498–502, Jun. 2006.
[36] A. S. Kurkov, "Q-switched all-fiber lasers with saturable absorbers," *Laser Phys. Lett.*, vol. 8, no. 5, pp. 335–342, Mar. 2011.
[37] S. D. Jackson, B. C. Dickinson, and T. A. King, "Sequence lasing in a gain-switched Yb^{3+},Er^{3+}-doped silica double-clad fiber laser, "*Appl. Opt.*, vol. 41, no. 9, pp. 1698–1703, Mar. 2002.
[38] J. Yang, Y. Tang, R. Zhang, and J. Xu, "Modeling and characteristics of gain-switched diode-pumped Er-Yb codoped fiber lasers," *IEEE J. Quantum Electron.*, vol. 48, no. 12, pp. 1560–1567, Dec. 2012.
[39] J. Yang, Y. Tang, and J. Xu, "Development and applications of gain-switched fiber lasers [Invited]," *Photon. Res.*, vol. 1, no. 1, pp. 52–57, Jun. 2013.